Green functions and associated sources in infinite and stratified poroelastic media

Claude Boutin, Guy Bonnet, Pierre-Yves Bard

Green functions and associated sources in infinite and stratified poroelastic media

C. Boutin[★†], G. Bonnet[★] and P. Y. Bard[‡§] [★]*Institut de Mécanique de Grenoble, BP 68, 38402 Saint-Martin-d'Hères Cedex, France;* [†]*Ecole Nationale des Travaux Publics de l'Etat, 69120 Vaulx-en-Velin, France;* [‡]*Laboratoire de Géophysique Interne et Tectonophysique, IRIGM, BP 68, 38402 Saint-Martin-d'Hères Cedex, France;* [§]*Laboratoire Central des Ponts-et-Chaussées, 58 Boulevard Lefebvre, 75732 Paris Cedex, France*

Summary. The purpose of this paper is to study Green functions for porous saturated media and to present an example of numerical simulation using these Green functions. In the first part the equations of the porous media are recalled and the principal results concerning the features of the waves are given. The second part is devoted to the determination of sources and Green functions. We give the analytical solution, then we study some of its properties. In the third part we focus on the construction of synthetic seismograms. We show examples of bi-dimensional computation in a semi-infinite stratified porous medium, for a double dipole or a fluid injection.

Key words: Green functions, sources, permeability, porous media, synthetic seismograms, P_2-wave

Introduction

The dynamics of porous saturated media was first developed by Biot (1956, 1962) using a phenomenological approach. More recently, the application of homogenization process to these materials (Auriault 1980; Auriault, Borne & Chambon 1985) has completed the Biot formulation and enables the computation of effective coefficients when the microstructure is periodic.

Many applications of Biot's theory have been proposed in various domains (seismic, acoustic, civil engineering). In the field of geophysics, the main contributions are those of Deresiewicz *et al.* (1960–67) and Geertsma & Smit (1961), which dealt with different plane-wave studies, Love and Rayleigh waves. Different analytical solutions were obtained by Mei & Foda (1981) using a boundary layer theory to solve wave propagation problems concerning civil and earthquake engineering. In the scope of full-wave acoustic logging, the work of Rosenbaum (1974) and Schmitt & Bouchon (1985) enabled synthetic siesmograms

in saturated porous formations to be obtained. The more specific subject of the determination of Green functions has already been studied by different authors (Burridge & Vargas 1979; Norris 1985; Bonnet 1987) but their solutions are either incomplete or unsatisfactory.

The purpose of this paper is to apply the results of homogenization theory, to study Green functions, which are very useful in solving complex problems with boundary integral techniques, and to present an example of numerical simulation of seismic tests in stratified soils.

In the first part, the equations of the porous saturated media are recalled and the principal features of the waves are given.

The second part is devoted to the determination of the sources and harmonic Green functions. We first present the theoretical method of resolution and give the analytical solution in the 2-D and 3-D cases. Then we exhibit a reciprocity theorem and introduce potentials corresponding to the different kinds of sources.

In the third part we focus on the construction of synthetic seismograms: we show examples of bi-dimensional computation in a semi-infinite stratified medium for a double dipole or a fluid injection. The important variation on the signal waveform with the permeability is shown to be attributed to the emission of the P_2 wave at the source. This result suggests the possibility of obtaining a permeability measurement from a simple seismic exploration.

1 The constitutive equations

1.1 BIOT THEORY

The main theory used for the description of saturated porous media is from Biot's study (1956). With the notations of Biot, the differential equations describing the motion of porous media are:

$$N u_{i,kk} + [(N+A)e + Q\epsilon]_{,i} - b(\dot{u}_i - \dot{U}_i) = \rho_{11}\ddot{u}_i + \rho_{12}\ddot{U}_i$$

$$(Qe + R\epsilon)_{,i} + b(\dot{u}_i - \dot{U}_i) = \rho_{12}\ddot{u}_i + \rho_{22}\ddot{U}_i \qquad i = 1, 3,$$

where A, N, Q, R are elastic coefficients, b is a viscous coupling term, and ρ_{ij} are inertial coupling parameters.

One essential problem in using Biot's theory is knowing what values have to be given to these coupling parameters. Important information is obtained on this subject by using the homogenization method.

1.2 COMPLEMENTS FROM HOMOGENIZATION METHOD

The homogenization theory for periodic structures (Auriault 1980; Auriault *et al.* 1985) leads to the following equations for the description of the harmonic behaviour of porous saturated media:

$$\underline{\underline{\Sigma}} = \underline{\underline{C}}\,\underline{\underline{e}}(\mathbf{U}_s) - \alpha P \underline{\underline{I}} \tag{1}$$

$$\operatorname{div}(\underline{\underline{\Sigma}}) = -\omega^2[\rho_s(1-n)\mathbf{U}_s + n\rho_l\mathbf{U}_l] \tag{2}$$

$$ni\omega(\mathbf{U}_l - \mathbf{U}_s) = \mathbf{K}(\omega)(\omega^2\rho_l\mathbf{U}_s - \operatorname{grad} P) \tag{3}$$

$$n \operatorname{div}(\mathbf{U}_l - \mathbf{U}_s) = -\alpha \operatorname{div}\mathbf{U}_s - \beta P \tag{4}$$

These equations assume that the medium is mechanically and geometrically isotropic, on the microscopic and macroscopic scales. The fluid is supposed to be viscous and Newtonian. $\underline{\Sigma}$ represents the total stress tensor; P represents the pressure (with the convention $P > 0$ in compression); $\mathbf{U}_s$ is the solid displacement; $\underline{e}(\mathbf{U}_s)$ the strain tensor, $\mathbf{U}_l$ is the fluid displacement; $\underline{C}$ is the elastic tensor of the skeleton; λ, μ the Lamé's coefficients; n is the porosity; $\alpha = 1 - K_b/K_s$, with K_b bulk compressibility such that $K_b = (3\lambda + 2\mu)/3$ and K_s solid compressibility; $\beta = (\alpha - n)/K_s + n/K_f$ with K_f fluid compressibility; and $\mathbf{K}(\omega)$, ω-dependent with a complex value, is the generalized Darcy coefficient introduced by the homogenization theory. In the case of unidirectional cylindrical ducts it can be shown that:

$$\mathbf{K}(\omega) = (i\mathbf{k})/(\nu\omega^*)J_2(\sqrt{-8i\omega^*})/J_0(\sqrt{-8i\omega^*}); \qquad \mathbf{k} = na^2/8; \quad \omega^* = \omega\mathbf{k}/n\nu$$

with J_0, J_2 being the Bessel functions, a the radius of the ducts, and ν the kinematic viscosity of the fluid.

This expression will be used for the calculation in the third part.

Remarks

Note that the inverse Fourier transform of the set of equations (1)–(4) leads to transient constitutive equations with a memory effect [due to the explicit frequency-dependent character of the coefficient $\mathbf{K}(\omega)$]. It is therefore more practicable to search for harmonic Green functions than for transient Green functions. We give in Table 1 the relations between all of these coefficients and Biot's coefficients.

Table 1. Relations between Biot's notations and homogenization notations.

Biot	A	N	M	Q	R	k	b(ω)	ρ_{22}
Homogenization	$\lambda + (\alpha - n)^2/\beta$	μ	$1/\beta$	$(\alpha - n)n/\beta$	n^2/β	$\nu\rho_l\mathbf{K}(0)$	$n^2\mathbf{H}_1(\omega)$	$n^2\mathbf{H}_2(\omega)/\omega$

1.3 EQUATIONS OF PROPAGATION

By elimination of $\underline{\Sigma}$ and P in equations (1)–(4) the propagation equations are obtained as below:

$$\left.\begin{aligned} &\mu\Delta\mathbf{U}_s + (\lambda + \mu)\,\mathbf{grad}\ \mathrm{div}\,(\mathbf{U}_s) = -\omega^2(\rho_{11}\mathbf{U}_s + \rho_{12}\mathbf{U}_l) + i\omega\eta(\mathbf{U}_s - \mathbf{U}_l) \\ &n\alpha/\beta\ \mathbf{grad}\ \mathrm{div}\,[(\alpha/n - 1)\mathbf{U}_s + \mathbf{U}_l] = -\omega^2(\rho_{21}\mathbf{U}_s + \rho_{22}\mathbf{U}_l) - i\omega\eta(\mathbf{U}_s - \mathbf{U}_l), \end{aligned}\right\} \quad (5)$$

strain energy — inertial terms — viscous dissipation

where

$$\mathbf{H} = \mathbf{H}_1 + i\mathbf{H}_2 = 1/\mathbf{K}(\omega)$$

with

$$\rho_{11} = (1 - n)\rho_s + \alpha(n\mathbf{H}_2/\omega - \rho_l)$$

$$\rho_{12} = n(\rho_l - \alpha\mathbf{H}_2/\omega) \qquad \eta = \alpha n\mathbf{H}_1$$

$$\rho_{21} = \alpha(\rho_l - n\mathbf{H}_2/\omega)$$

$$\rho_{22} = \alpha n\mathbf{H}_2/\omega.$$

This set of equations (5), connecting the strain energy with the inertial terms and the viscous dissipation, is similar to Biot's set of equations (Biot 1956, 1962).

The characteristic frequency F_c, defined by:

$$F_c = \frac{\nu n}{\mathbf{k} \cdot 2\pi}$$

separates the low-frequency range ($f \ll F_c$), where the viscous terms are greater than the intertial terms, and the high-frequency range ($f \ll F_c$), where, conversely, the viscous terms are negligible with respect to the inertial terms.

1.4 WAVES IN POROUS SATURATED MEDIUM

Using Helmholtz theorem, the fields of solid and fluid displacements can be written in the form:

$$\left.\begin{aligned} \mathbf{U}_s &= \mathbf{grad}\,(\Phi_s) + \mathbf{curl}\,(\Psi_s) \qquad \operatorname{div}(\Psi_s) = 0 \\ \mathbf{U}_l &= \mathbf{grad}\,(\Phi_l) + \mathbf{curl}\,(\Psi_l); \qquad \operatorname{div}(\Psi_l) = 0 \end{aligned}\right\}. \tag{6}$$

Substituting these expressions in equation (5) we get the following differential equations:

the scalar potential satisfies: $(\Delta + \delta_1^2)(\Delta + \delta_2^2)\Phi = 0$;

the vector potential satisfies: $(\Delta + \delta_3^2)\Psi = 0$,

which means that there are two compressional waves P_1 and P_2 and one shear wave S, having $\delta_1, \delta_2, \delta_3$, respectively, as wavenumbers.

It may also be shown that the potentials of the fluid displacements are related to the potentials of solid displacements by multiplicator coefficients μ_1, μ_2, μ_3, respectively, for the P_1, P_2 and S waves. That is:

$$\left.\begin{aligned} \mathbf{U}_s &= \mathbf{grad}\,(\Phi_1) + \mathbf{grad}\,(\Phi_2) + \mathbf{curl}\,(\Psi) \\ \mathbf{U}_l &= \mu_1\,\mathbf{grad}\,(\Phi_1) + \mu_2\,\mathbf{grad}\,(\Phi_2) + \mu_3\,\mathbf{curl}\,(\Psi) \end{aligned}\right\}. \tag{7}$$

The expression of these wave numbers δ_i and coefficients μ_i involves the elastic coefficients and the complex permeability $\mathbf{K}(\omega)$.

Therefore they are also ω-dependent and complex valued. Consequently there is an attenuation and a dispersion for the three waves (Biot 1956). Lastly, the calculation shows that fluid and solid displacements are practically in phase opposition for the P_2 wave.

2 Harmonic Green functions in infinite porous saturated medium

Green functions in porous saturated media have already been studied by different authors: Burridge & Vargas (1979) give a transient solution in far field, only for point forces; Norris (1985) introduces point forces in the fluid, which is shown by Bonnet (1986) to be unsatisfactory; Bonnet (1986) provides an harmonic solution by analogy with the thermo-elasticity, but this solution does not allow clear identification of the sources involved in the calculation. Our new formulation presents the following advantages:

We give the physical meaning for each kind of source;
The symmetry of the Green matrix leads to a reciprocity theorem;
The solution is valid at any frequency, for any distance.

2.1 INDEPENDENT VARIABLES IN THE POROUS MEDIUM

The determination of Green functions is practicable only if we use independent variables. Taking into account the fact that $\mathbf{U}_s$ and $\mathbf{U}_f$ can always be written in the form of equation (7), it can be seen that the six components of the displacements are not independent. In fact, we deduce from this system that there are only four degrees of freedom [corresponding to Φ_1, Φ_2 and two components of Ψ because of div $(\Psi) = 0$].

Therefore, we choose the solid displacement $\mathbf{U}_s$ and the pressure P as independent variables to describe the behaviour of the porous medium.

2.2 POINT EXCITATION AND DIFFERENTIAL SYSTEM

Green functions are the response of the medium to point excitations. To seek these fundamental solutions, we have to add to the set of local equations (1)–(4) four perturbations corresponding to the four degrees of freedom. Throughout this study we focus on monochromatic behaviour, and consequently the excitations are assumed to be harmonic.

These perturbations will necessarily appear in the balance equations, that is, in the dynamic equation (2) we add a vectorial quantity $\boldsymbol{F}\delta|x|\exp(i\omega t)$ which is the force density corresponding to an harmonic point-force located at the origin and applied to the skeleton ($\delta|x|$ being the Dirac distribution), and in the continuity equation (4) we introduce a scalar term $V\delta|x|\exp(i\omega t)$ which is the volume density corresponding to an harmonic punctual volume injected ($V > 0$) at the origin.

Thus, a porous medium undergoing the harmonic sources $\boldsymbol{F}$ and V located at the origin is described by the foregoing set of equations, where the time factor $\exp(i\omega t)$ has been omitted:

$$\underline{\underline{\Sigma}} = \underline{\underline{C}}\,\underline{\underline{e}}(\mathbf{U}_s) - \alpha P \underline{\underline{I}}$$

$$\text{div}\,(\underline{\underline{\Sigma}}) = -\omega^2\,[\rho_s(1-n)\,\mathbf{U}_s + n\rho_f\mathbf{U}_f] - \boldsymbol{F}\delta|x|$$

$$ni\omega(\mathbf{U}_f - \mathbf{U}_s) = \mathbf{K}(\omega)\,(\omega^2\rho_f\mathbf{U}_s - \mathbf{grad}\,P)$$

$$n\,\text{div}\,(\mathbf{U}_f - \mathbf{U}_s) = -\alpha\,\text{div}\,\mathbf{U}_s - \beta P - V\delta|x|.$$

In order to solve this differential system we eliminate the variables $\mathbf{U}_f$ and $\underline{\underline{\Sigma}}$. We obtain the following system involving the independent variables $\mathbf{U}_s$ and P

$$\left.\begin{aligned}&(\lambda+\mu)\,\mathbf{grad}\,\text{div}\,(\mathbf{U}_s) + \mu\Delta\mathbf{U}_s + \omega^2\mathring{\rho}\mathbf{U}_s - \mathring{\alpha}\,\mathbf{grad}\,P = -\boldsymbol{F}\delta|x|\\&\theta\Delta P - \beta P - \mathring{\alpha}\,\text{div}\,(\mathbf{U}_s) = -V\delta|x|,\end{aligned}\right\} \tag{8}$$

where

$$\mathring{\rho} = (1-n)\rho_s + \rho_f\,[n + \rho_f\omega^2\mathbf{K}(\omega)/i\omega]\,; \qquad \theta = \mathbf{K}(\omega)/i\omega$$

$$\mathring{\alpha} = \alpha + \rho_f\omega^2\mathbf{K}(\omega)/i\omega.$$

Let $\boldsymbol{S}$ be the four-component solicitation vector:

$$\boldsymbol{S}\left|\begin{matrix}\boldsymbol{F}\\V\end{matrix}\right.,$$

and $\boldsymbol{R}$ the four-component response vector:

$$\boldsymbol{R}\left|\begin{matrix}\mathbf{U}_s\\P\end{matrix}\right..$$

Equation (8) can thus be put in the form:

$$\underline{\underline{B}}\,R + S\delta\,|x| = 0,$$

where $\underline{\underline{B}}$ is the differential operator defined by:

$$B_{ij} = \left((\lambda+\mu)\frac{\partial^2}{\partial x_i \partial x_j} + \delta_{ij}\mu(\Delta + \omega^2 \mathring{\rho})\right)(1-\delta_{i4})(1-\delta_{j4}) + \mathring{\alpha}\left(\delta_{i4}\frac{\partial}{\partial x_j} + \delta_{j4}\frac{\partial}{\partial x_i}\right)$$

$$\times(\delta_{i4}\delta_{j4} - 1) + (\theta\Delta - \beta)\,\delta_{i4}\delta_{j4},$$

with δ_{ij} being the Kronecker symbol; $i, j = 1, 4$ in the 3-D case. In the 2-D case, i, j are running from 1 to 3.

Note that the $\underline{\underline{B}}$ matrix is symmetrical which is related to the reciprocity theorem shown in Section 2.5.

2.3 DETERMINATION OF THE BASIS SOLUTIONS: THE METHOD

The problem is to find the matrix $\underline{\underline{G}}(4*4)$ solution of:

$$\underline{\underline{B}}\,\underline{\underline{G}} + \underline{\underline{I}}\,\delta\,|x| = 0$$

$\underline{\underline{I}}$ being the unity matrix, or

$$\underline{\underline{B}}\,g_k + s_k\delta\,|x| = 0 \qquad k, i = 1, 4; \quad g_{ki} = G_{ki}; \quad s_{ki} = \delta_{ki}, \tag{9}$$

where g_k is the response vector to the unit solicitation s_k.

To obtain the different elements of the matrix $\underline{\underline{G}}$ we use the Kupradze method (Kupradze 1979), which enables us to determine the sixteen – or nine in a 2-D case – functions G_{ki} from a single unknown function φ:

Consider the differential operator $\underline{\underline{B}}'$ built from the cofactors of $\underline{\underline{B}}$. We have:

$$\underline{\underline{B}}\,\underline{\underline{B}}' = \mathrm{DET}\,(\underline{\underline{B}})\underline{\underline{I}}$$

Let us now assume that φ is the scalar solution to the equation

$$\mathrm{DET}\,(\underline{\underline{B}})\varphi + \delta\,|x| = 0 \tag{10}$$

and that φ satisfies also the condition:

$$[\mathrm{DET}\,(\underline{\underline{B}})\underline{\underline{I}}]\,\varphi + \delta\,|\,x\,| \simeq 0$$

which gives:

$$\underline{\underline{B}}(\underline{\underline{B}}'\varphi) + \underline{\underline{I}}\,\delta\,|x| = 0.$$

Consequently, in comparison with equation (9) we get:

$$\underline{\underline{G}} = \underline{\underline{B}}'\varphi.$$

In conclusion, $\underline{\underline{G}}$ is obtained by applying the differential operator $\underline{\underline{B}}'$ to the function φ. In our case, the computation of the cofactors leads to:

$$\underline{\underline{B}}' = \underline{\underline{B}}''\mu(\Delta + \delta_3^2) \quad \text{and} \quad \mathrm{DET}\,(\underline{\underline{B}}) = \mu(\Delta + \delta_3^2)D, \tag{11}$$

where

$$B''_{ij} = \left(-\frac{\partial^2}{\partial x_i \partial x_j} [(\lambda + \mu)(\theta\Delta - \beta) - \mathring{\alpha}^2] + \delta_{ij}\theta(\lambda + 2\mu)(\Delta + \delta_1^2)(\Delta + \delta_2^2) \right)(1 - \delta_{i4})(1 - \delta_{j4})$$

$$+ \mu(\Delta + \delta_3^2)\left[-\mathring{\alpha}\left(\delta_{i4}\frac{\partial}{\partial x_j} + \delta_{j4}\frac{\partial}{\partial x_i} \right)(\delta_{i4}\delta_{j4} - 1) + [(\lambda + 2\mu)\Delta + \mu\delta_3^2]\delta_{i4}\delta_{j4} \right]$$

$$D = \mu(\lambda + 2\mu)\theta(\Delta + \delta_3^2)(\Delta + \delta_2^2)(\Delta + \delta_3^2). \qquad (12)$$

In the 2-D case we get $\underline{B}'(3^*3)$ by substituting in B''_{ij} the Kronecker symbols δ_{i4}, δ_{j4} by the symbols δ_{i3}, δ_{j3}, i, j being run from 1 to 3 and we have DET $(\underline{B}) = D$.

2.4 FUNDAMENTAL SOLUTION

We have to find the solution φ of equation (10). However, because of relations (11) the problem reduces to the determination of χ, solution of:

$$\underline{B}(\underline{B}''\chi) + \delta\,|\,x\,|\,\underline{I} = (D\chi + \delta\,|\,x\,|)\,\underline{I} = 0.$$

On the other hand, because of the expression (12) of D, if ξ satisfies the equation:

$$(\Delta + \delta_1^2)(\Delta + \delta_2^2)(\Delta + \delta_3^2)\xi + \delta|x| = 0,$$

it can be seen that:

$$\chi = \xi/\theta\mu(\lambda + 2\mu).$$

By looking for ξ in the form

$$\xi = \sum_{i=1}^{3} a_i \xi_i,$$

where

$$(\Delta + \delta_i^2)\xi_i + \delta|x| = 0 \qquad i = 1, 3,$$

we obtain, after computation,

$$a_i = (\delta_{i+1}^2 - \delta_{i+2}^2)/\Pi; \quad \Pi = (\delta_1^2 - \delta_3^2)(\delta_2^2 - \delta_1^2)(\delta_3^2 - \delta_2^2); \quad \text{with } \delta_{i+3}^2 = \delta_i^2$$

which implies that:

$$\chi = \sum_{i=1}^{3} \xi_i(\delta_{i+1}^2 - \delta_{i+2}^2)/(\lambda + 2\mu)\mu\theta\Pi.$$

The solutions ξ_i of Helmholt's equations corresponding to the three waves P_1, P_2 and S are well-known functions: in the 3-D case: $\xi_j = \exp(-i\delta_j\,|\,x\,|)(1/4\pi\,|\,x\,|)$; in the 2-D case: $\xi_j = H_0^2(\delta_j\,|\,x\,|)(1/4i)$, H_0^2 being the Hankel's function of zero order.

By applying the operator $\underline{B}''$ to χ, we get the Green matrix. Below we give this expression in 2-D and 3-D cases.

3-D case

$$G_{ij} = \frac{1}{4\pi}\left[\left[-\left(\sum_{k=1}^{3} \alpha_k \exp(-i\delta_k |x|)/|x|\right)_{,ij} + \frac{\delta_{ij}}{\mu} \exp(-i\delta_3 |x|)/|x|\right](\delta_{i4}-1)(\delta_{j4}-1)\right.$$

$$+\left[\delta_{j4}\left(\sum_{k=1}^{2} \xi(-1)^k \exp(-i\delta_k |x|)/|x|\right)_{,i} + \delta_{i4}\left(\sum_{k=1}^{2} \xi(-1)^k \exp(-i\delta_k |x|)/|x|\right)_{ij}\right]$$

$$\left.\times(\delta_{i4}\delta_{i4}-1) - \frac{1}{\theta\alpha_3}[\alpha_2 \exp(-i\delta_1 |x|)/|x| + \alpha_1 \exp(-i\delta_2 |x|)/|x|]\,\delta_{i4}\delta_{j4}\right] \quad (13)$$

2-D case

$$G_{ij} = \frac{1}{4\pi}\left[\left[-\left(\sum_{k=1}^{3} \alpha_k H_0^2(\delta_k |x|)\right)_{,ij} + \frac{\delta_{ij}}{\mu} H_0^2(\delta_3 |x|)\right](\delta_{i3}-1)(\delta_{j3}-1)\right.$$

$$-\frac{\delta_{i3}\delta_{j3}}{\theta\alpha_3}[\alpha_2 H_0^2(\delta_1 |x|) + \alpha_1 H_0^2(\delta_2 |x|)] + \left[\delta_{j3}\left(\sum_{k=1}^{2} \xi(-1)^k H_0^2(\delta_k |x|)\right)_{,i}\right.$$

$$\left.\left.+\,\delta_{i3}\left(\sum_{k=1}^{2} \xi(-1)^k H_0^2(\delta_k |x|)\right)_{,j}\right](\delta_{i3}\delta_{j3}-1)\right] \quad (14)$$

with

$\alpha_1 = (\delta_2^2 - \mu\delta_3^2/(\lambda+2\mu)/\mu\delta_3^2(\delta_2^2-\delta_1^2)$ $\qquad \zeta = 1/n(\mu_1-\mu_2)$

$\alpha_2 = [\delta_1^2 - \mu\delta_3^2/(\lambda+2\mu)]/\mu\delta_3(\delta_1^2-\delta_2^2)$ $\qquad \theta = \mathbf{K}(\omega)/i\omega$

$\alpha_3 = -1/\mu\delta_3^2$.

Note that the Green matrix is symmetric, as is the $\underline{\underline{B}}$ matrix.

2.5 PHYSICAL INTERPRETATION

2.5.1 Reciprocity theorem

The main characteristic of the Green matrix is its symmetry. This property corresponds to a reciprocity theorem.

Let us consider the two loadings represented in Fig. 1. Here we have:

$$\boldsymbol{R}_1 = \underline{\underline{G}}|x_N - x_M|\boldsymbol{S}_1; \quad \boldsymbol{R}_2 = \underline{\underline{G}}|x_M - x_N|\boldsymbol{S}_2.$$

Note that:

$$\xi_{i,j}|x_N - x_M| = -\xi_{i,j}|x_M - x_N|$$

and

$$\xi_{i,jk}|x_N - x_M| = +\xi_{i,jk}|x_M - x_N|; \qquad i,j,k = 1,3,$$

which means that:

$$G_{ij}|x_N - x_M| = G_{ij}|x_M - x_N|(-1)^{\delta_{i4}+\delta_{j4}}; \qquad i,j = 1,4. \quad (15)$$

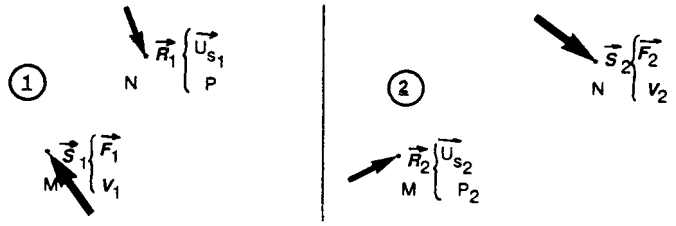

Figure 1. Reciprocity theorem: the two different loadings of the porous saturated medium.

Compute now the coupled work:

$$W = \mathbf{U}_{s1} F_2 - P_1 V_2 ,$$

$$W = G_{ij} |x_N - x_M| (S_1)_j (S_2)_i (-1)^{\delta_{i4}} ;$$

using the symmetry of the matrix and relation (14), W can be changed to:

$$W = G_{ij} |x_M - x_N| (-1)^{\delta_{i4} + \delta_{j4}} (S_2)_i (S_1)_j (-1)^{\delta_{i4}}$$

$$W = G_{ij} |x_M - x_N| (S_2)_i (S_1)_j (-1)^{\delta_{j4}} .$$

Finally we obtain:

$$W = \mathbf{U}_{s1} F_2 - P_1 V_2 = \mathbf{U}_{s2} F_1 - P_2 V_1 .$$

This equality gives a direct demonstration in infinite porous saturated media of a reciprocity theorem which was already introduced by Predeleanu (1984) using an integral formulation.

2.5.2 Features of the potentials

Let us come back to the Green matrix. The expression of the displacements enables us to determine the potentials:

Harmonic point force

It appears from equations (13 and 14) that the solid displacements generated by a unit force in the k-direction are given by:

$$(\mathbf{U}_{sk})_i = -\left(\sum_{j=1}^{3} \alpha_j \xi_j \right) + (\xi_3/\mu)\delta_{ik}$$

which can also be written as:

$$\mathbf{U}_{sk} = \mathbf{grad}\,[-(\alpha_1 \xi_1)_{,k}] + \mathbf{grad}\,[-(\alpha_2 \xi_2)_{,k}] + \mathbf{curl}\,[\mathbf{e}_k \wedge \mathbf{grad}\,(\alpha_3 \xi_3)] ,$$

where $\mathbf{e}_k$ is the unitary vector in the k-direction. In terms of potentials we get:

$\Phi_1 = -(\alpha_1 \xi_1)_{,k}$ $\quad$ P_1-wave

$\Phi_2 = -(\alpha_2 \xi_2)_{,k}$ $\quad$ P_2-wave

$\Psi = \mathbf{e}_k \wedge \mathbf{grad}\,(\alpha_3 \xi_3)$ $\quad$ S-wave.

Note that the displacements are cylindrically symmetric around the direction of the force in the 3-D case and only plane symmetrical around that direction in the 2-D case.

Now consider the pressure P_k. We have:

$$P_k = -\zeta(\xi_1 - \xi_2)_{,k}. \tag{16}$$

The contribution of S-waves in the pressure is obviously zero. P_k satisfies the same symmetry condition as the displacements.

Another way to get the pressure P_k is to introduce the expression of the displacements $\mathbf{U}_{sk}$ into equation (4). Thus we get:

$$P_k = -(\xi_1)_{,k}[n(\mu_1 - 1) + \alpha]\alpha_1\delta_1^2/\beta - (\xi_2)_{,k}[n(\mu_2 - 1) + \alpha]\alpha_2\delta_2^2/\beta,$$

and by identification with (16) we deduce the following relations:

$$[n(\mu_1 - 1) + \alpha]\alpha_1\delta_1^2/\beta = -[n(\mu_2 - 1) + \alpha]\alpha_2\delta_2^2/\beta = 1/(\mu_1 - \mu_2)n = \zeta. \tag{17}$$

Harmonic volume source

Under this solicitation the solid displacements are:

$$(\mathbf{U}_{s4})_i = -\zeta(\xi_1 - \xi_2)_{,i},$$

which implies that:

$$\mathbf{U}_{s4} = -[\mathbf{grad}\,(\zeta\xi_1) - \mathbf{grad}\,(\zeta\xi_2)].$$

Thus the potentials are:

$\Phi_1 = -\zeta\xi_1$ $\quad P_1$-wave

$\Phi_2 = +\zeta\xi_2$ $\quad P_2$-wave

$\Psi = 0$ $\quad S$-wave.

Consequently there is no shear wave in the field radiated by a volume source. The displacements present a spheric symmetry – or radial in the 2-D case – centred on point source.

The pressure is given by:

$$P_4 = -(\alpha_2\xi_1 + \alpha_1\xi_2)/(\alpha_3\theta).$$

Using the same procedure as in the preceding section we obtain the relations:

$$\zeta\delta_1^2[n(\mu_1 - 1) + \alpha]/\beta = \alpha_2/(\alpha_3\theta); \qquad \zeta\delta_2^2[n(\mu_2 - 1) + \alpha]/\beta = -\alpha_1/(\alpha_3\theta)$$

which leads, by combination with relation (17), to the identity:

$$[n(\mu_1 - 1) + \alpha][n(\mu_2 - 1) + \alpha] = -\beta(\lambda + 2\mu). \tag{18}$$

Harmonic doublet

In elastic media, explosions are formally represented by double dipoles (for 2-D problems) or triple dipoles (for 3-D problems). For such a source, also called 'doublets' the distribution of forces is:

$$\mathbf{grad}\,\delta|x|.$$

An expression can be found for the potentials by deriving the potentials obtained for a point force.

Thus:

$$\Phi_j = -\sum_{k=1}^{3} (\Phi_j)_{,k} = \sum_{k=1}^{3} (\alpha_j \xi_j)_{,kk} = \alpha_j \Delta \xi_j = -\alpha_j (\delta_j^2 \xi_j - \delta \mid x \mid); \qquad j = 1, 2$$

$$\Psi = -\sum_{k=1}^{3} (\Psi^k)_{,k} = -\sum_{k=1}^{3} [\![\mathbf{curl}\ [\mathbf{e}_k \wedge \mathbf{grad}\ (\alpha_3 \xi_3)]]\!]_{,k} = -\mathbf{curl}\ \left[\!\!\left[\sum_{k=1}^{3} [\mathbf{e}_k \wedge \mathbf{grad}\ (\alpha_3 \xi_3)]_{,k} \right]\!\!\right]$$

$$\Psi = -\mathbf{curl}\ \mathbf{curl}\ \mathbf{grad}\ (\alpha_3 \xi_3) = 0.$$

Thus:

$\Phi_1 = -\alpha_1 \delta_1^2 \xi_1 + \alpha_1 \delta \mid x \mid$ $\quad P_1$-wave

$\Phi_2 = -\alpha_2 \delta_2^2 \xi_2 + \alpha_2 \delta \mid x \mid$ $\quad P_2$-wave

$\Psi = 0$ $\quad S$-wave.

As in the elastic case there are no shear waves and the spherical (3-D) or radial symmetry (2-D) is still satisfied.

Remarks: (i) In porous saturated media there are two different kinds of sources which radiate only compressional waves. (ii) By combinations of fluid injection and doublets, it is possible to generate either only one P_2-wave or only one P_1-wave.

2.6 DECOMPOSITION OF WAVEFIELD IN 'ELEMENTARY' WAVES

It is useful to have a decomposition of the radiated field in 'elementary' waves which have well-known properties.

In the 3-D case

We can use the Sommerfield integral to introduce a decomposition in cylindrical waves:

$$\exp(-i\delta \mid x \mid)/4\pi \mid x \mid = \int_0^\infty J_0(kr) \exp(-i\gamma x_1) k/i\gamma \, dk \tag{19}$$

with

$$\mid x \mid^2 = x_1^2 + r^2; \qquad \gamma = \sqrt{\delta^2 - k^2}; \qquad \mathrm{Re}\,(\gamma) > 0$$

In the 2-D case

The inverse Fourier transform of Hankel functions leads to a decomposition in plane-waves:

$$H_0^2(\delta \mid x \mid)/4i = \int_{-\infty}^{\infty} \exp(-ikx_1) \exp(-i\gamma x_2)/i\gamma \, dk \tag{20}$$

with

$$\mid x \mid^2 = x_1^2 + x_2^2; \qquad \gamma = \sqrt{\delta^2 - k^2}; \qquad \mathrm{Re}\,(\gamma) > 0.$$

Deriving this expression under the sign $\int$ with respect to the spatial variables and substituting them in Green matrix, we obtain the decomposition of the wavefield in

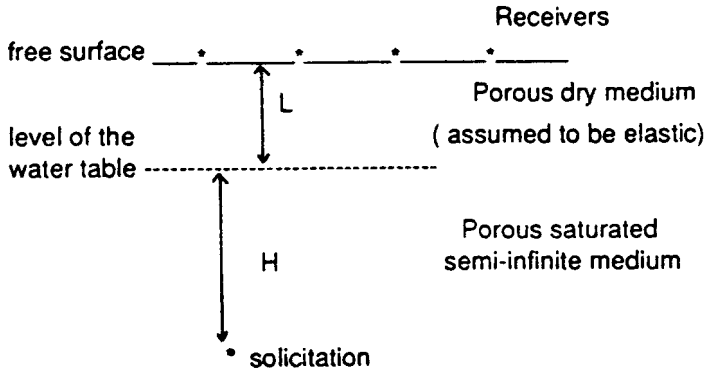

Figure 2. Geometrical configuration of the 2-D study.

'elementary' waves. This formulation is very well adapted to calculations by using the discrete wavenumber method (Bouchon 1980).

3 Application: calculation of synthetic seismograms (2-D case)

In this section we deal with the numerical simulation of harmonic pumpings or seismic *in situ* tests: we apply our results to the calculation of synthetic seismograms when the solicitation – a double dipole or a volume extraction – is located in the saturated medium. We treat the 2-D configuration described in Fig. 2.

The response of sandstone and sand have been studied. The mechanical characteristics of these materials are given in Table 2, and we can find in Figs 3 and 4 the variation of the velocities of the waves against the dimensionless frequency $f^* = f/F_c$. We varied the permeability between 10^{-10} and 5×10^{-9} m^2. These values correspond to very permeable soils and would represent a very fissured rock in the case of sandstone.

3.1 METHOD OF COMPUTATION: DISCRETIZATION OF GREEN FUNCTIONS

Green functions are first computed in the frequency domain by using the discrete wavenumber method (Bouchon 1980) from which we recall the basic principle.

Let us consider on point M in an infinite medium, the response $B_\omega(OM)$ to an harmonic

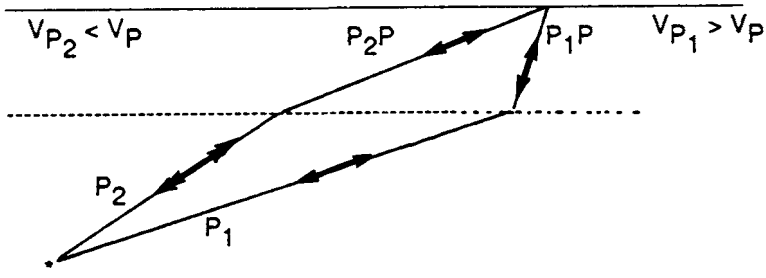

Figure 3. Effects of the contrasts of velocities on the rays of PP_1 and PP_2 waves.

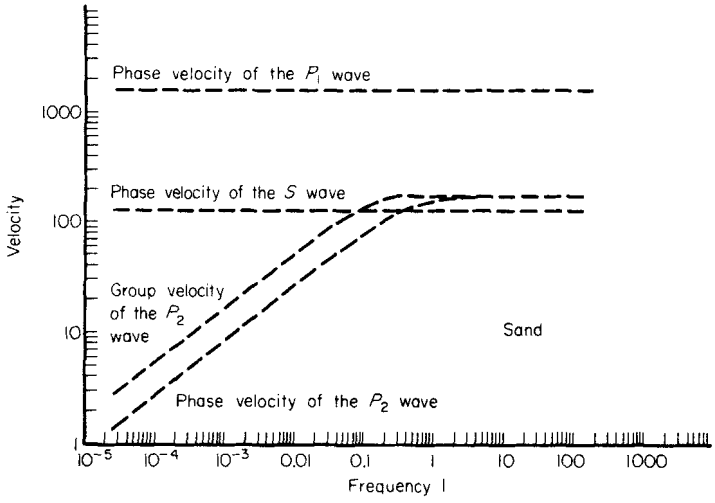

Figure 4. Dispersion of the velocities for the sandstone.

Table 2. Mechanical characteristics of the sandstone and the sand.

Coefficients (U.S.I.)	E	ν	ρ_s	K_s	n	ρ_f	η	K_f
Sand	10^8	0.3	2700	$3.6\,10^{11}$	0.3	1000	10^{-3}	210^9
Sandstone	310^9	0.2	2700	$3.6\,10^{11}$	0.2	1000	10^{-3}	210^9

solicitation $\boldsymbol{S}_\omega$ located at the origin. $\boldsymbol{R}_\omega(OM)$ can be expressed with its inverse spatial Fourier transform $\boldsymbol{R}_\omega(k, x_2)$ in the form:

$$\boldsymbol{R}_\omega(OM) = \int_{-\infty}^{\infty} \exp(-ikx_1)\, \boldsymbol{R}_\omega(k, x_2)\, dk \qquad x_1^2 + x_2^2 = |x|^2.$$

Assuming now a L-periodic array of such a solicitation in the Ox_1 direction, the response $\boldsymbol{R}_\omega(M)$ will also be L-periodic in the Ox_1 direction and we have:

$$\boldsymbol{R}_\omega(M) = \sum_{j=-\infty}^{\infty} \boldsymbol{R}_\omega(O_jM) = \sum_{j=-\infty}^{\infty} \int_{-\infty}^{\infty} \exp[-ik(x_1 - jL)]\, \boldsymbol{R}_\omega(k, x_2)\, dk,$$

i.e.

$$\boldsymbol{R}_\omega(M) = \int_{-\infty}^{\infty} \exp(-ikx_1)\, \boldsymbol{R}_\omega(k, x_2) \sum_{j=-\infty}^{\infty} \exp(-ikjL)\, dk$$

but

$$\sum_{j=-\infty}^{\infty} \exp(-ikjL) = 2\pi/L \sum_{j=-\infty}^{\infty} \delta(k - 2\pi j/L);$$

thus

$$\boldsymbol{R}_\omega(M) = \sum_{j=-\infty}^{\infty} \exp(-ik_j x_1)\, \boldsymbol{R}_\omega(k_j, x_2)\, \Delta k; \qquad \Delta k = 2\pi/L; \quad k_j = j\Delta k.$$

This result shows that a periodic arrangement of sources identical to each other radiates energy in only discrete directions (Bouchon 1980). This remark implies that, for a L-periodic source array in the Ox_1 direction, the continuous superposition of plane-waves given in equation (20) becomes an infinite discrete summation. In our case, the function $\boldsymbol{R}_\omega(k_j, x_2)$ is deduced from equations (14) and (20).

To return to the temporal domain we use the time Fourier transform.

The spatial periodization of the structure and the inverse-time Fourier transform introduce numerical perturbations which can be removed by using a complex frequency and adapting L with the studied time-window (for more details see Bouchon 1980).

3.2 RADIATED FIELD IN LAYERED MEDIUM

When the source – a double dipole or a fluid injection – is located in the layered media, we first discretize the wavefield in P_1 and P_2 plane-waves as in an infinite medium, and then propagate each of these plane-waves through the dry layer. Consequently, for P_1 and P_2 plane-waves and for each propagation direction determined by the horizontal wavenumber $k_j = j\Delta k$, we have to find the amplitudes and phases of the transmitted and reflected plane-waves generated at the interfaces.

We obtain these transmission coefficients by solving the system of interface conditions, i.e.:

On the top of the water-table the continuity of the tractions and the displacements and the zero value of the pressure (for more details see Dutta & Ode 1983).

On the free surface the zero value of the stress.

On a point $M(x_1)$ on the free surface, the displacement generated by the P_n plane-wave

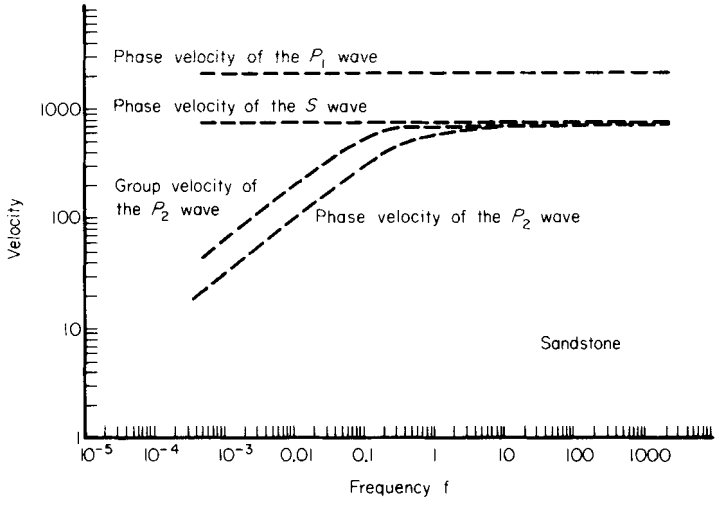

Figure 5. Dispersion of the velocities for the sand.

$(n = 1, 2)$ with a horizontal wavenumber $k_j = j\Delta k$ is therefore given in the generic form:

$$u_{nj}(x_1) = \exp(ik_j x_1)\, g_n(k_j) \exp(i\omega\eta_j H) \left[P_{nj}\overleftarrow{P} \exp(i\gamma_j L) + P_{nj}\overrightarrow{P} \exp(-i\gamma_j L) + P_{nj}\overleftarrow{S} \exp(i\nu_j L) + P_{nj}\overrightarrow{S} \exp(-i\nu_j L)\right], \tag{21}$$

where $g_n(k_j)$ is given by the Green functions and depends on: (i) the kind of source; (ii) the wave considered (P_1 or P_2); (iii) the direction of displacement.

η_j, γ_j, ν_j are, respectively, the vertical wave numbers of the P_{nj} wave (in the saturated medium), P and S waves (in the dry elastic medium) associated with the horizontal wave number $k_j = j\Delta k$.

$P_{nj}\overleftarrow{P}$, $P_{nj}\overrightarrow{P}$, $P_{nj}\overleftarrow{S}$, $P_{nj}\overrightarrow{S}$, are the transmission coefficients (in potential) of the different waves in the dry layer, for an incident P_{nj} wave from the saturated medium with an horizontal wave number k_j.

Finally, by summation over the horizontal wave number, and again over the kind of wave radiated by the source (only P_1 and P_2 in our case), we get, for a given frequency, on the point $M(x_1)$ on the free surface:

$$\mathbf{u}(x_1) = \sum_{j=-\infty}^{\infty} \sum_{n=1}^{2} \mathbf{u}_{nj}(x_1).$$

The value of M is determined, for each frequency, by a convergence criterion.

3.3 RESULTS AND INTERPRETATION

We choose as time variation of the source, a Ricker wavelet whose central frequency is $f_{\text{source}} = 200$ Hz.

The synthetic seismograms are plotted in Figs 6–9 for the sand and in Figs 10–17 for the sandstone.

3.3.1 Response to a double dipole (Figs 6–13)

We note that the form of the seismograms is strongly dependent on the permeability. In particular, when the frequency of the source is smaller than the characteristic frequency F_c the seismograms consist of only early arrivals (Figs 6 and 10). Inversely for a source frequency such that $f_{\text{source}} > F_c$ there appears a second pulse (Figs 7, 9, 11 and 13).

The first arrival obviously corresponds to the fastest wave, that is P_1P. Because of the great contrast between the dry and saturated media, this wave is accompanied by a train of interreflected PP waves in the case of sand (Figs 6 and 7). The attenuation of these waves when the permeability increases, i.e. when f^* increases, is due to the fact that the intrinsic attenuation of the P_1 wave increases with the frequency. Consequently, for the medium and high frequency ranges (i.e. $f^* > 1$) a homogeneous P_1-wave will be converted to a strongly attenuated inhomogeneous P_1P-wave.

The last arrival also corresponds to a compressional wave (both the horizontal and vertical displacements are in phase). This pulse is identified as the P_2P-wave, for the following reasons:

(a) We have computed the hodochrone for the P_2P-wave in the layered media corresponding to Fig. 8. For this calculation we first determine the group and phase velocity of the P_2-wave at the central frequency of the source; then the time arrival is computed by using the group velocity in the saturated medium and the phase velocity for the deviation of

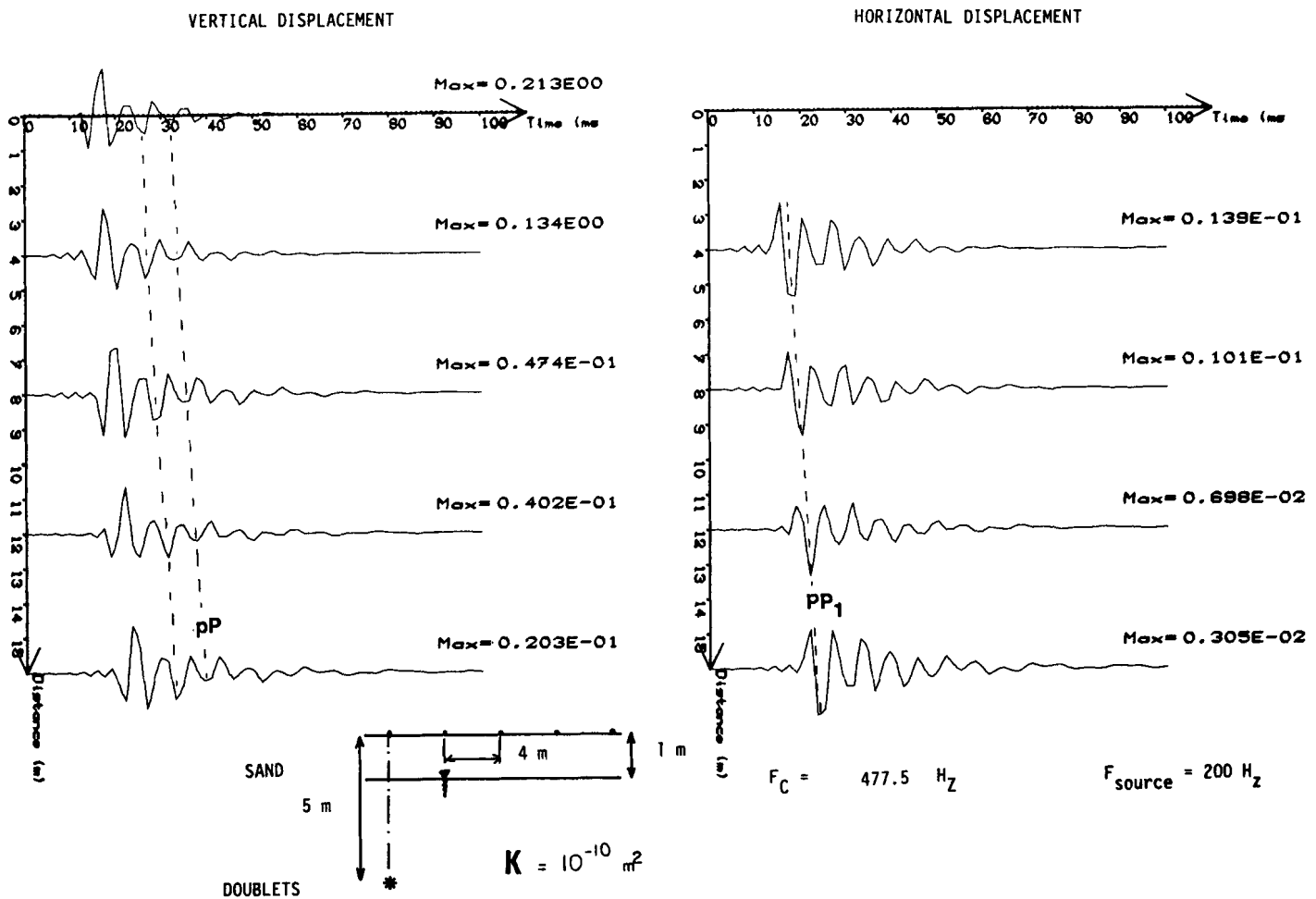

Figure 6. Seismograms for a doublets source in sand. Permeability $k = 10^{-10}$ m^2.

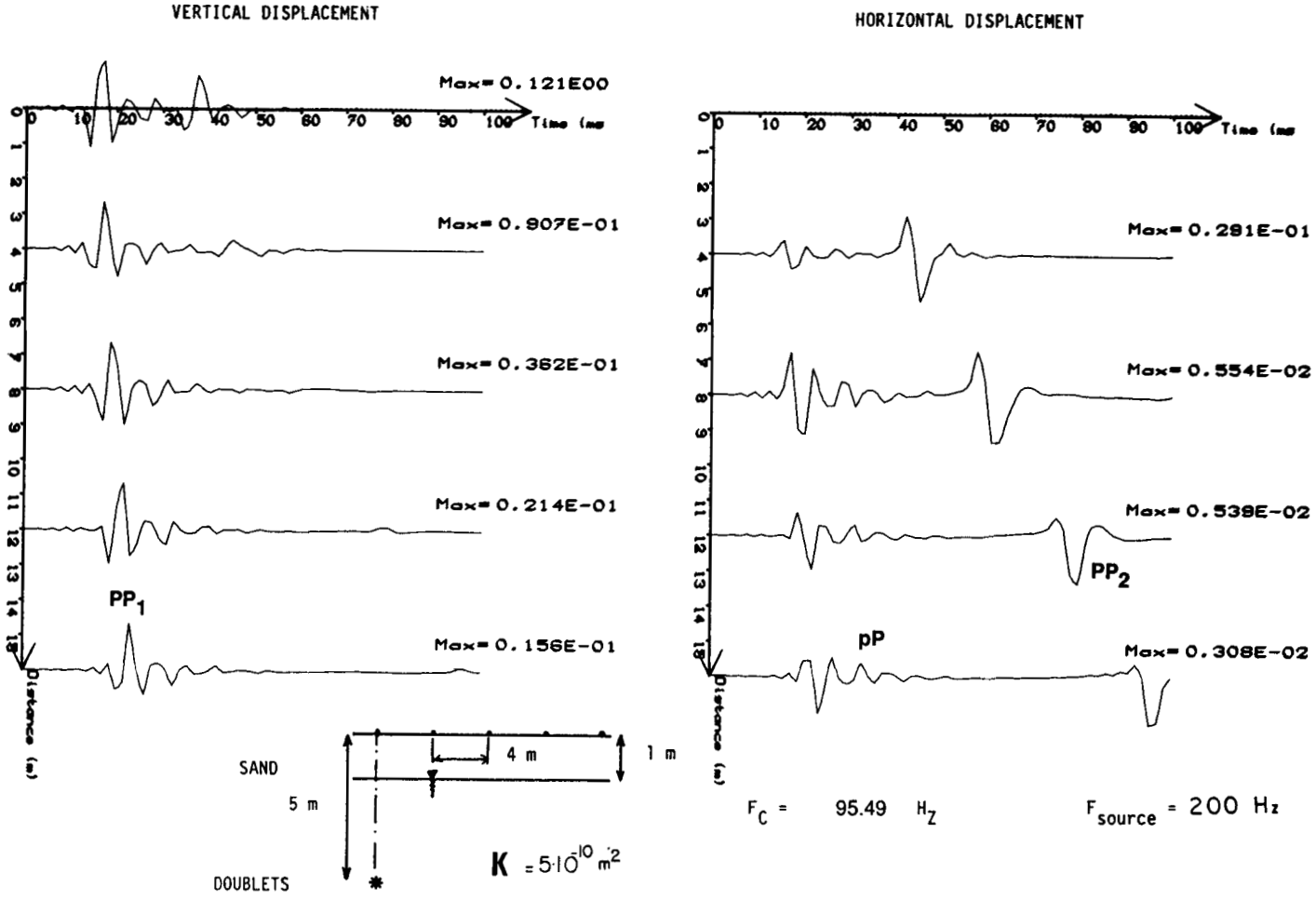

Figure 7. Seismograms for a doublets source in sand. Permeability $\mathbf{k} = 5 \times 10^{-10}$ m^2.

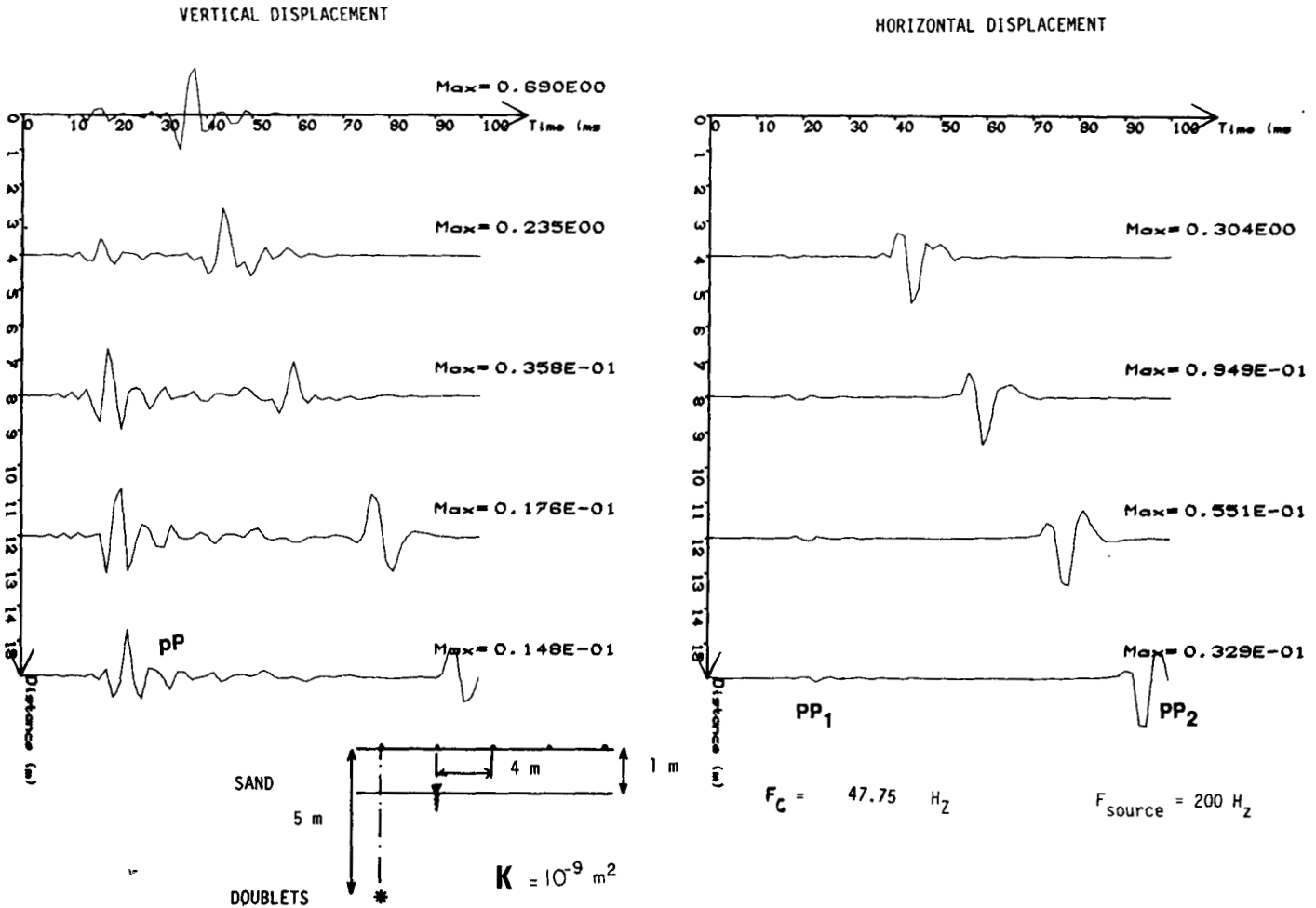

Figure 8. Seismograms for a doublets source in sand. Permeability $k = 5 \times 10^{-9}$ m².

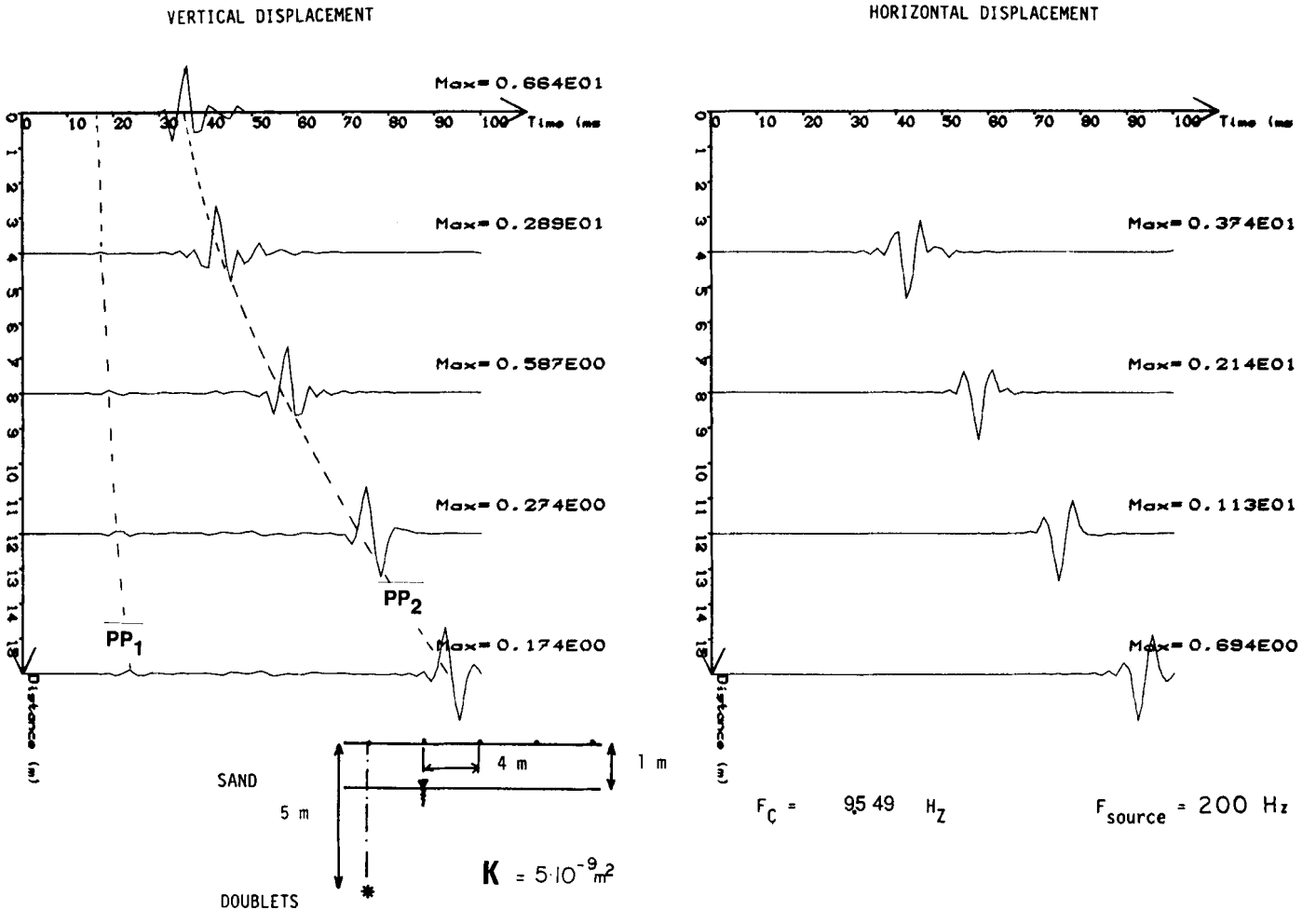

Figure 9. Seismograms for a doublets source in sand. Permeability $\mathbf{k} = 5 \times 10^{-9}$ m^2.

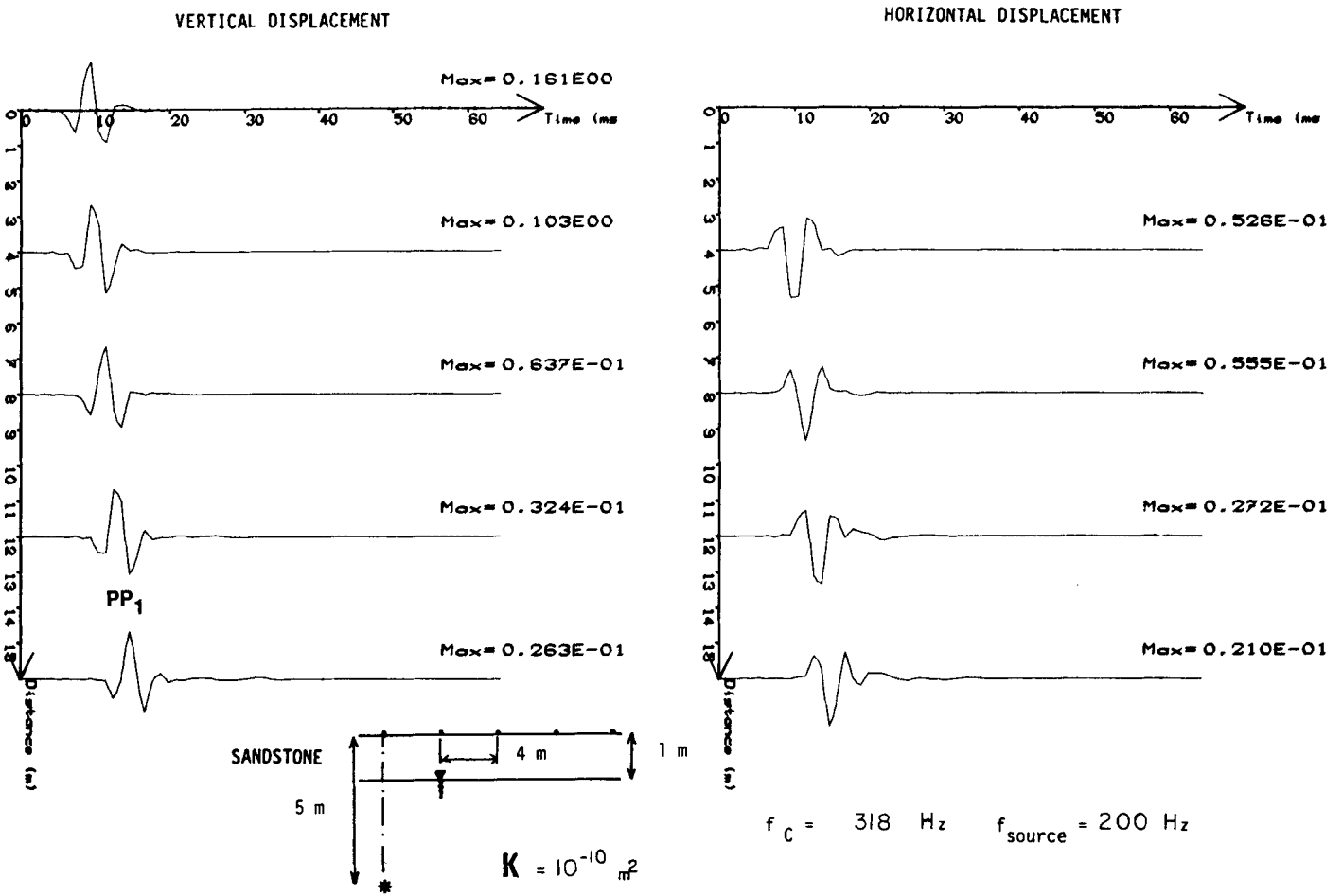

Figure 10. Seismograms for a doublets source in sandstone. $\mathbf{k} = 10^{-10}\ \mathrm{m}^2$.

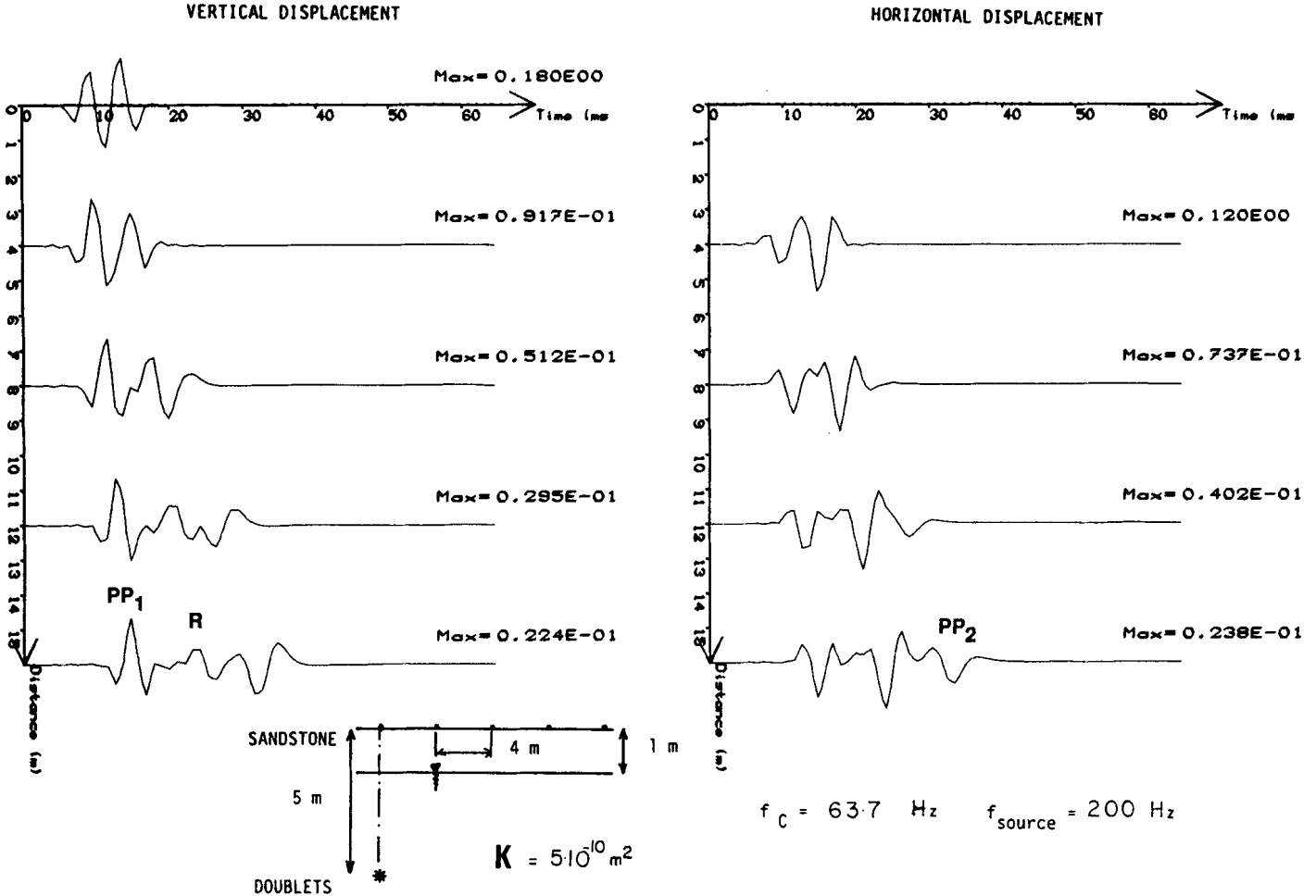

Figure 11. Seismograms for a doublets source in sandstone. $\mathbf{k} = 5 \times 10^{-10}$ m^2.

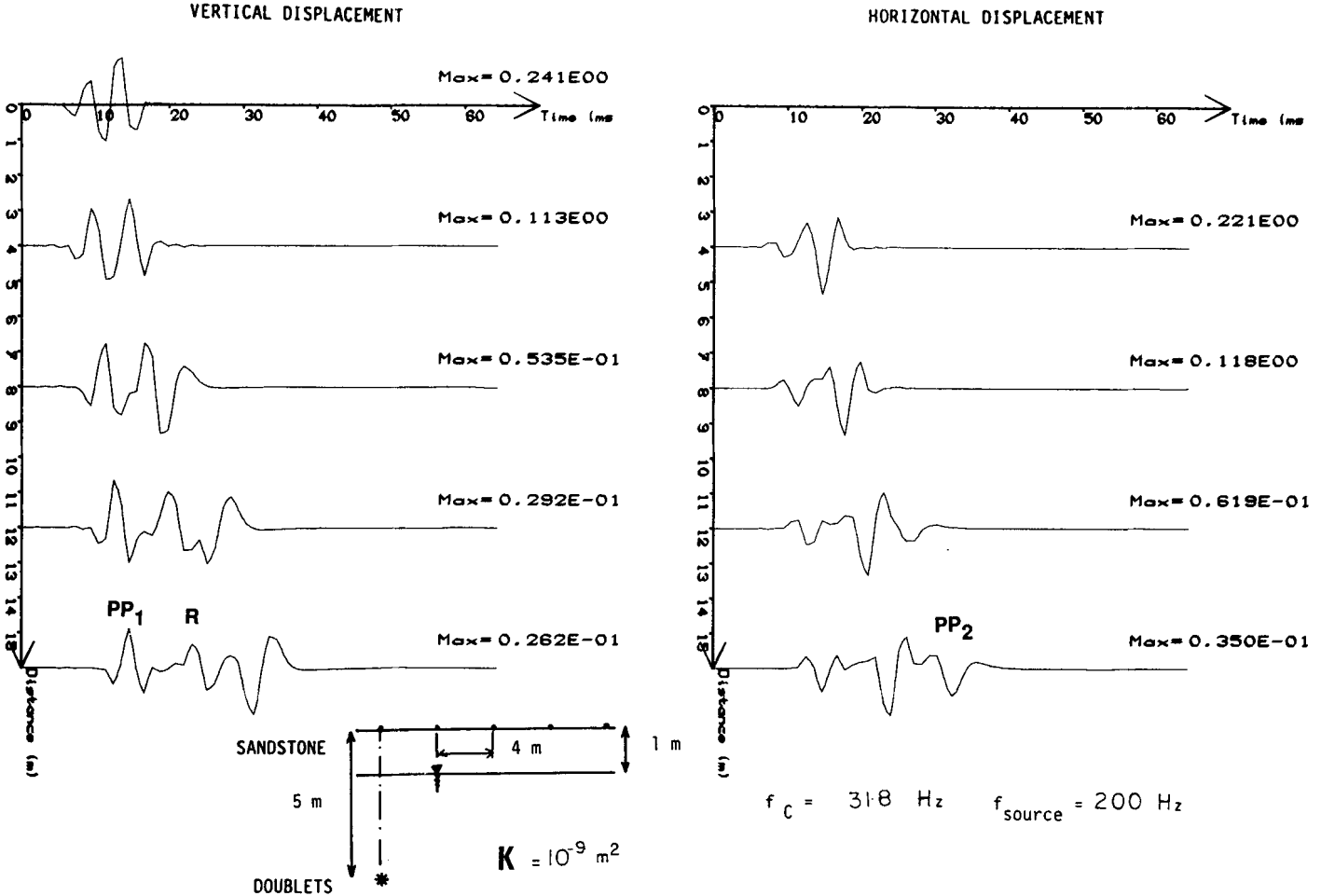

Figure 12. Seismograms for a doublets source in sandstone. $\mathbf{k} = 10^{-9}$ m^2.

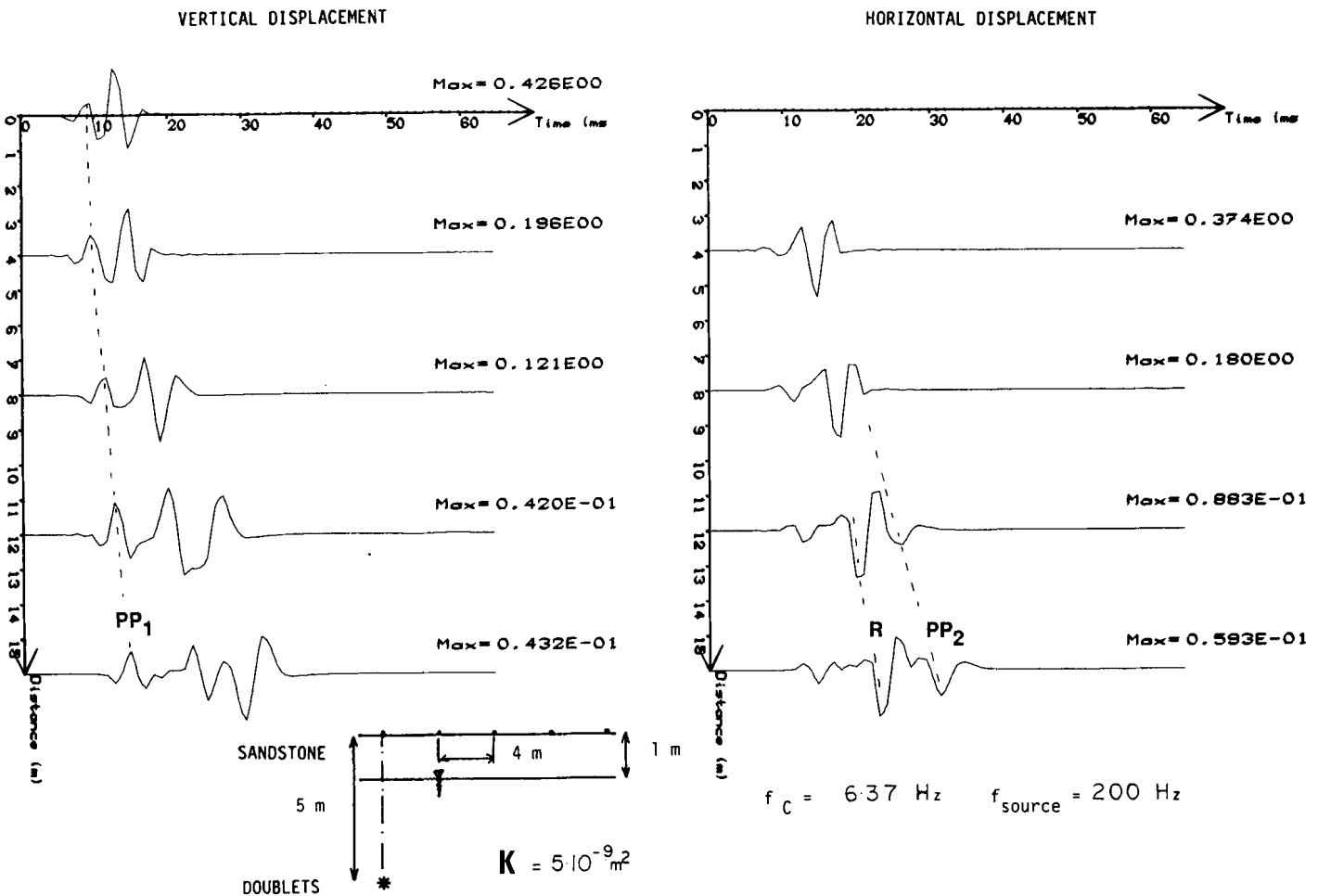

Figure 13. Seismograms for a doublets source in sandstone. $\mathbf{k} = 5 \times 10^{-9}$ m².

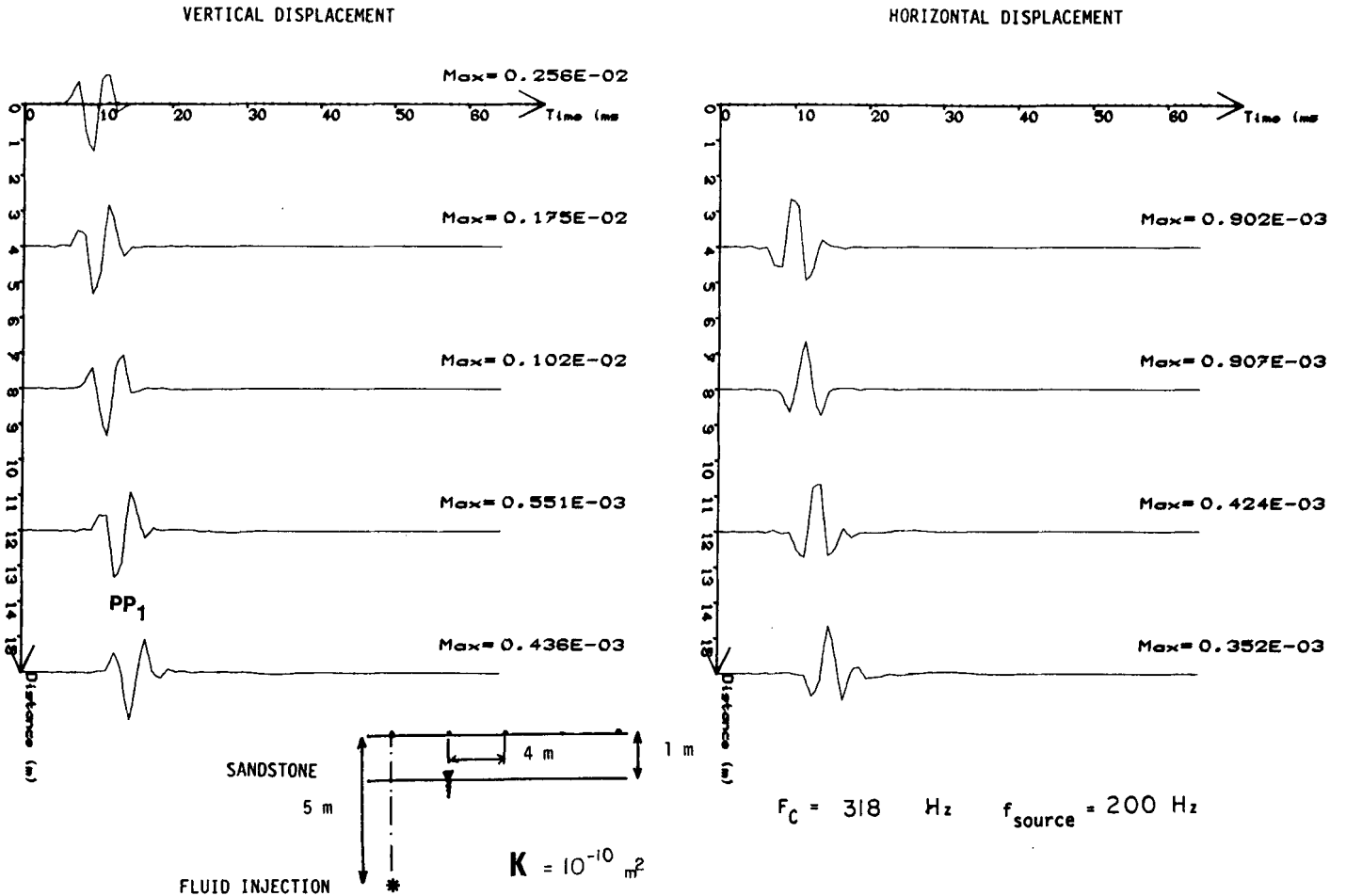

Figure 14. Seismograms for a volume source in sandstone. $k = 10^{-10}\ m^2$.

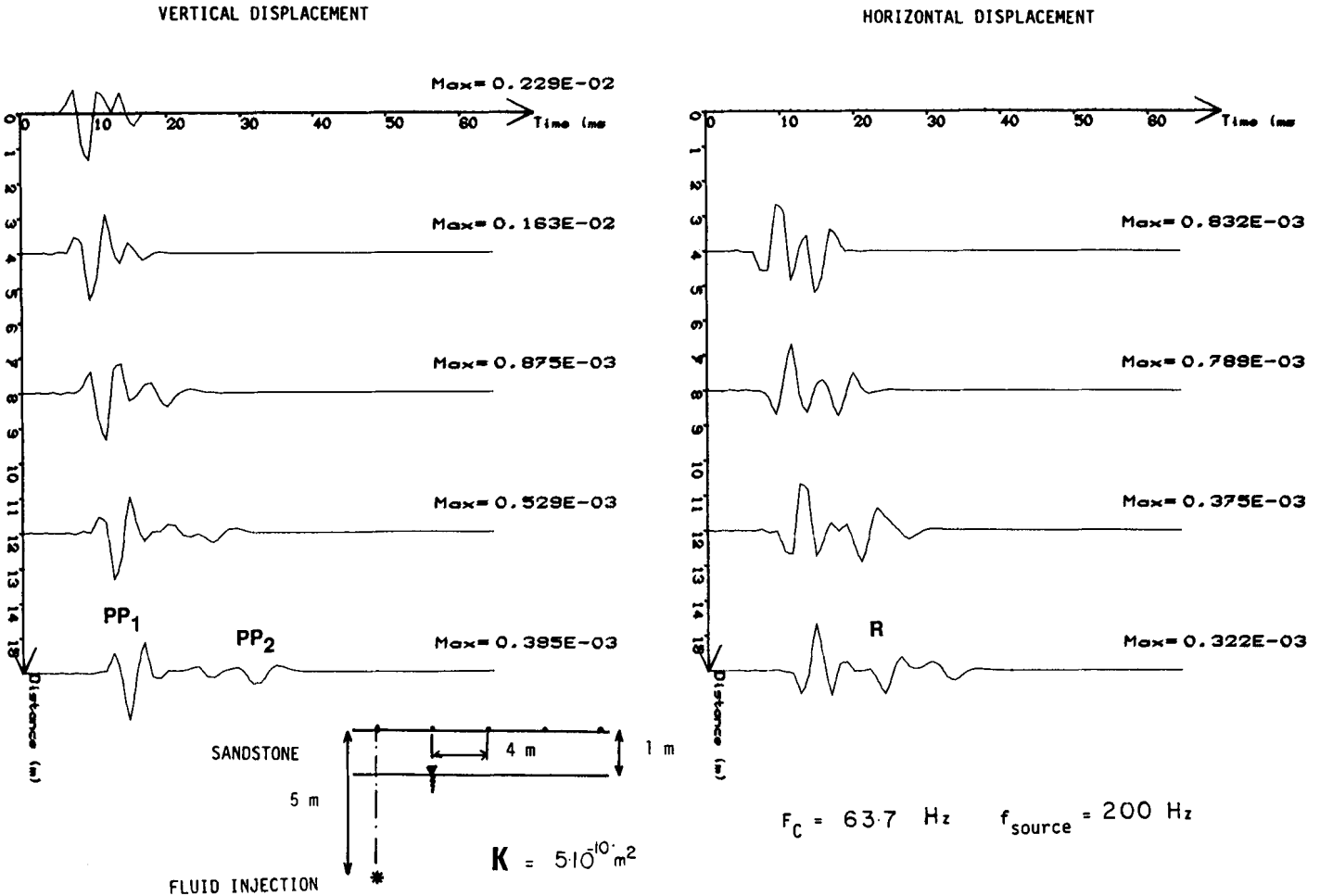

Figure 15. Seismograms for a volume source in sandstone. $\mathbf{k} = 5 \times 10^{-10}$ m^2.

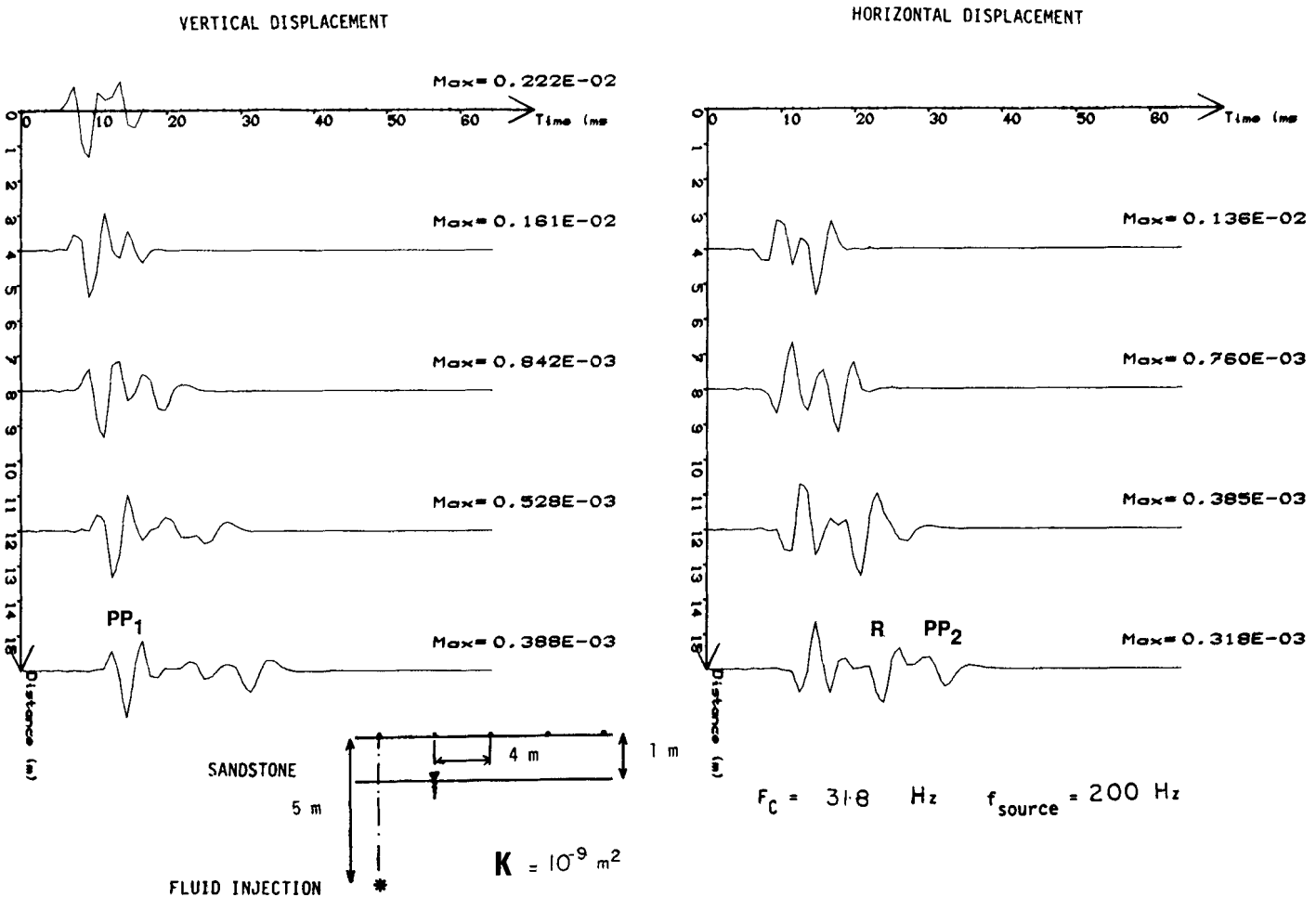

Figure 16. Seismograms for a volume source in sandstone. $k = 10^{-9}$ m^2.

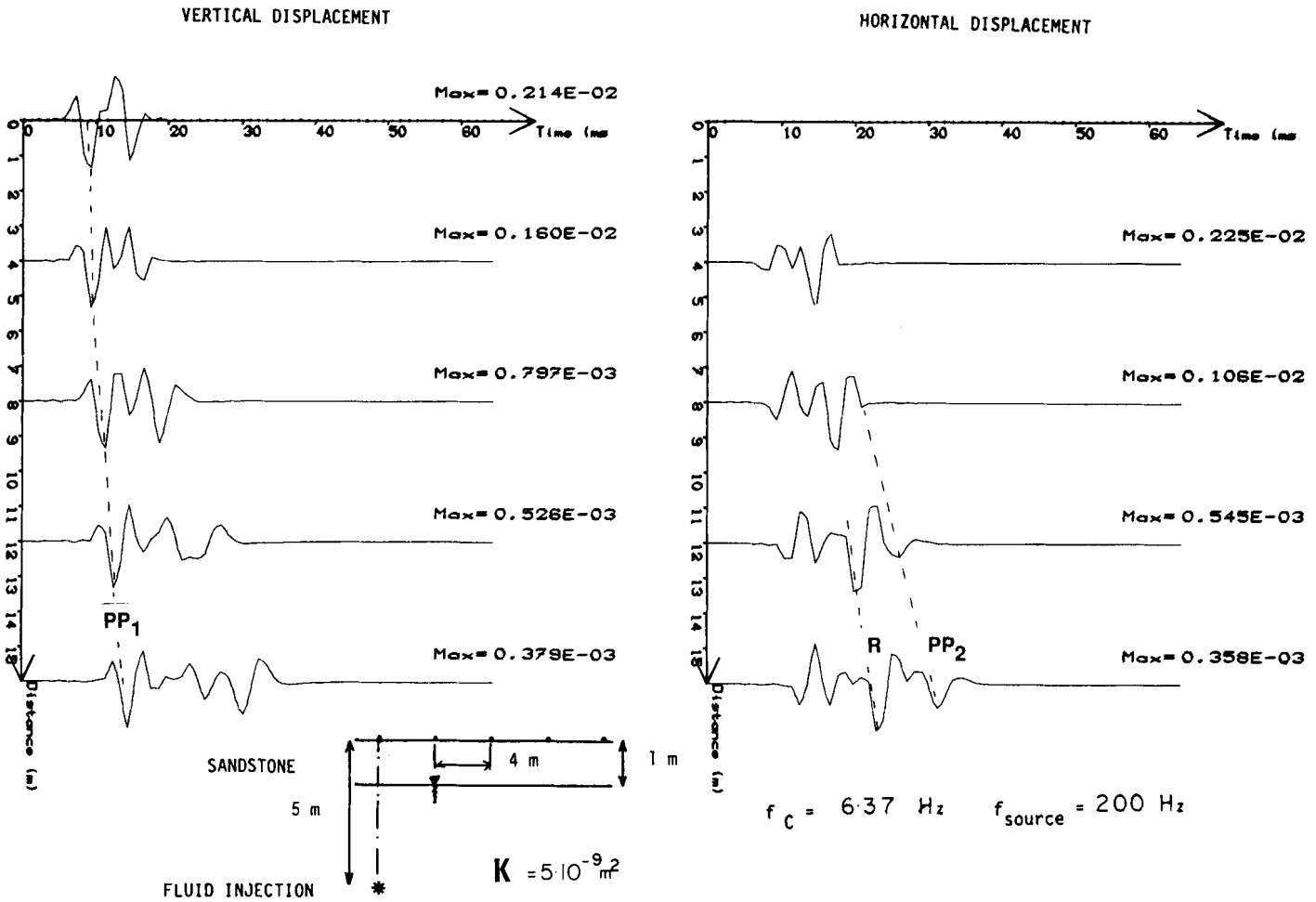

Figure 17. Seismograms for a volume source in sandstone. $k = 5 \times 10^{-9}$ m².

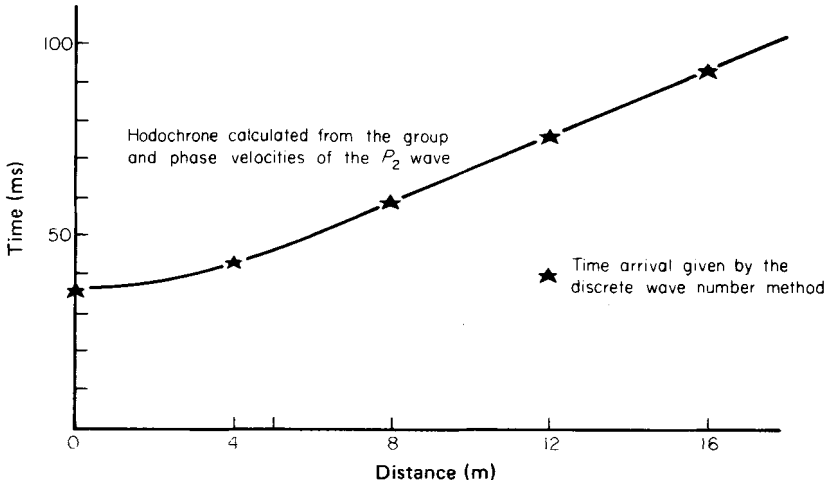

Figure 18. Hodochrone of the PP_2-wave in the case of Fig. 8.

the ray due to Descartes's law at the interface. Comparison with the hodochrone obtained by the discrete wave number method shows a very good agreement (Fig. 18).

(b) The P_2P-wave has a strong horizontal component which can be explained by the contrasts of the velocities (see Fig. 3).

(c) The decrease in the P_2P-amplitude with distance is much larger than for the amplitude of P_1P.

In all the cases the vanishing of the P_2P-wave for the weak permeabilities, i.e. for small f^*, is explained by the specific behaviour of the P_2-wave at low frequencies: (i) the P_2-velocity vanishes as frequency tends to zero; (ii) the P_2 attenuation is very strong with respect to that of P_1; (iii) the P-wave transmitted from an incident P_2-wave is very inhomogeneous in the low-frequency range.

At last we can observe in Figs 9 and 13, for points far away from the source, the apparition of a third pulse between the P_1P and P_2P arrivals. Because there is a phase shift of $\pi/2$ between the horizontal and the vertical displacements, this wave probably corresponds to an interface mode.

3.3.2 Response to fluid injection (Figs 14–17)

The study of the seismograms shows that, in this case, the previous analysis is still applicable. However, if we compare with the case of a doublets source, we note an amplitude difference and a phase shift of π between the P_1P and the P_2P waves. We can explain these observations by comparing the potentials generated by the two kinds of sources:

We see in Section 2.5.2 that a volume source creates the following potentials:

$$\Phi_1 = \zeta\xi_1, \quad \Phi_2 = -\zeta\xi_2;$$

by using the relations (17) we can also say that:

$$\Phi_1 = \alpha_1\delta_1^2[n(\mu_1 - 1) + \alpha]/\beta\xi_1; \quad \Phi_2 = \alpha_2\delta_2^2[n(\mu_2 - 1) + \alpha]/\beta\xi_2.$$

On the other hand, the potentials generated by a doublet source are:

$$\Phi_1 = -\alpha_1\delta_1^2\xi_1 + \alpha_1\delta|x|; \quad \Phi_2 = -\alpha_2\delta_2^2\xi_2 + \alpha_2\delta|x|.$$

That is, except for the solicitation point:

$$\Phi_1 = -\alpha_1 \delta_1^2 \xi_1 ; \quad \Phi_2 = -\alpha_2 \delta_2^2 \xi_2 .$$

Thus, in comparison with the case of doublets, the relative amplitude P_2P/P_1P for a volume source is multiplied by a complex coefficient C which is given by:

$$C = (\mu_2 - 1 + \alpha/n)/(\mu_1 - 1 + \alpha/n).$$

It can be shown that C tends to the negative real value $-(\lambda + 2\mu)\beta/\alpha^2$ when the frequency vanishes; and the calculation proves that the value of C stays almost constant over the whole range of frequencies.

In the case of the sandstone we have $C = -0.443$ which explains the phase shift of π and the differences in relative amplitudes.

Lastly, when the compressibility of the fluid is smaller than the compressibility of the solid ($K_f \gg K_b$), it is interesting to note that the absolute value of C satisfies the inequality $|C| < 1$, which means that the P_2-wave appears stronger with a doublet source than with a volume source.

Conclusion

Using the results of the homogenization theory for periodic structures, we have presented a new analytical formulation for the Green matrix in porous saturated media. These results allow us to make calculations in such media by using either the boundary integral-equation technique or the discrete wave-number method.

The presentation of seismograms from a doublet or a volume source provides an illustration of the results obtained by these Green functions.

This simple result does show that the signal waveform is strongly dependent on the permeability value (above a permeability level of about $10^{-10}\,m^2$, i.e. 100 Darcy). An immediate consequence is the possibility of obtaining permeability measurements with simple seismic explorations.

Acknowledgments

This research was supported by the ATP 'Propagation of waves in heterogeneous and fissured media', of the French Centre National de la Recherche Scientifique.

References

Auriault, J. L., 1980. Dynamic behaviour of a porous medium saturated by a Newtonian fluid, *Int. J. Engng. Sci.*, **18**, 775–785.

Auriault, J. L., Borne, L. & Chambon, R., 1985. Dynamics of porous saturated media; checking of the generalized law of Darcy, *J. acoust. Soc. Am.*, 77, 1641–1650.

Biot, M. A., 1956. Theory of propagation of elastic waves in a fluid saturated porous solid. I. Low frequency range. II. Higher frequency range, *J. acoust. Soc. Am.*, **28**, 168–191.

Biot, M. A., 1962. Generalized theory of acoustic propagation in porous dissipative media, *J. acoust. Soc. Am.*, **34**, 1254–1264.

Bonnet, G., 1987. Basic singular solutions and boundary integral equations for a poroelastic medium in the dynamic range, *J. acoust. Soc. Am.* (submitted).

Bouchon, M., 1980. Calculation of complete seismograms for an explosive source in a layered medium, *Geophysics*, **45**, 197–203.

Burridge, R. & Vargas, C. A., 1979. The fundamental solution in dynamic poroelasticity, *Geophys. J. R. astr. Soc.*, **58**, 61–90.

Deresiewicz, H. *et al.* 1960–1967. Effects of boundaries on wave propagation in liquid filled porous solid (I–X), *Bull. seism. Soc. Am.*, 50–57.

Dutta, N. C. & Ode, 1983. Seismic reflection from a gas water contact, *Geophysics*, **48**, 148–162.

Geertsma, J. & Smit, D. C., 1961. Some aspects of elastic wave propagation in fluid saturated porous solids, *Geophysics*, **26**, 169–181.

Kupradze, V. D., 1979. *Three-dimensional Problems of the Mathematical Theory of Elasticity and Thermoelasticity*, North-Holland, Amsterdam.

Mei, C. C. & Foda, M. A., 1981. Wave-induced responses in a fluid-filled poroelastic solid with a free surface. A boundary-layer theory, *Geophys. J. R. astr. Soc.*, **66**, 597–631.

Norris, A. N., 1985. Radiation from a point source and scattering theory in a fluid saturated porous solid, *J. acoust. Soc. Am.*, **77**, 2012–2023.

Predeleanu, M., 1984. Development of boundary element method to dynamic problems for porous media, *Appl. Math. Modelling*, **8**, 378–382.

Rosenbaum, J., 1974. Synthetic seismogram: logging in porous formation, *Geophysics*, **39**, 14–32.

Schmitt, D. P. & Bouchon, M., 1985. Full wave acoustic logging: synthetic microseismograms and frequency wavenumber analysis, *Geophysics*, **50**, 1756–1778.